University of Nebraska - Lincoln
DigitalCommons@University of Nebraska - Lincoln

Faculty Publications in Computer & Electronics Engineering (to 2015)

Electrical & Computer Engineering, Department of

7-2011

Quantifying Performance of Cooperative Diversity using the Sampling Property of a Delta Function

Won Mee Jang
University of Nebraska - Lincoln, wjang1@unl.edu

Follow this and additional works at: http://digitalcommons.unl.edu/computerelectronicfacpub

 Part of the Computer Engineering Commons

Jang, Won Mee, "Quantifying Performance of Cooperative Diversity using the Sampling Property of a Delta Function" (2011). *Faculty Publications in Computer & Electronics Engineering (to 2015)*. 77.
http://digitalcommons.unl.edu/computerelectronicfacpub/77

This Article is brought to you for free and open access by the Electrical & Computer Engineering, Department of at DigitalCommons@University of Nebraska - Lincoln. It has been accepted for inclusion in Faculty Publications in Computer & Electronics Engineering (to 2015) by an authorized administrator of DigitalCommons@University of Nebraska - Lincoln.

Quantifying Performance of Cooperative Diversity using the Sampling Property of a Delta Function

Won Mee Jang

***Abstract*—In this paper, we present a simple approach to evaluating the performance of amplify-and-forward cooperative diversity. The Q-function can be asymptotically reduced to a delta (impulse) function. We extend the result to cooperative networks in fading channels. The proposed approach introduces a simple technique to evaluate the performance of complex networks by sampling.**

***Index Terms*—Cooperative diversity, amplify-and-forward, delta function, sampling.**

I. Introduction

COOPERATIVE diversity (CD) was introduced in [1], [2]. The relays either decode and retransmit the received signal, called decode and forward (DF), or simply amplify and forward (AF) the signal. In [3], the asymptotic symbol error probability of AF-CD is derived in Rayleigh fading channels. Multi-hop relaying with AF over Nakagami-m fading channels has been studied in [4], [5]. Cooperative diversity networks have been investigated under Nakagami-m fading for AF-CD [6] and DF-CD [7]. The bit error rate (BER) analysis of dual-hop AF-CD is presented with maximal-ratio-combining (MRC) in [8] and selection-combining (SC) in [9]. Most of the analysis involves an integration of the conditional error probability with the channel fading probability density function (PDF) obtained from the moment generating function (MGF) to determine the performance bound. However, the performance analysis of a CD network is not straightforward, and often provides results only for limited forms of network. In this paper, we propose a new method to obtain the performance of a general AF-CD network using the sampling property of a delta function. We approximate the Q-function with a delta impulse function to obtain the novel BER expression.

II. Derivation

We consider the AF-CD with MRC in general fading channels. The two-relayed cooperative system is shown in Fig. 1 where x_1 (or y_1), x_2 (or y_2), x_3 (or y_3) and z denote the instantaneous power of the fading from the source (S) to the relay (R), R to R, R to the destination (D), and S to D, respectively, with the unit average power of the fading in the direct path. The average power of x_i or y_i may not vary independently due to physical limitations of the propagation path-loss effect between terminals. For the optimal relay placement, relays should be equally spaced between S and D, and we obtain [3, Eq. (24)]

$$E\left[|x_i|^2\right] = h^p E\left[|z|^2\right] \text{ or } E\left[|y_i|^2\right] = h^p E\left[|z|^2\right] \tag{1}$$

where $E\left[|\cdot|^2\right]$ indicates the average power, and h and p are the number of hops and the path-loss exponent, respectively. The subchannels are orthogonal in adjacent time slots or frequencies. We choose the amplification factor A to maintain the constant average power output equal to the original transmitted power,

$$A^2 = \frac{P_x}{P_x x + \sigma^2}, \tag{2}$$

where P_x is the transmitted power at S, and $\sigma^2 = N_o/2$ is the two-sided noise power spectral density. x is the instantaneous power of the fading. The general approach to evaluating communication systems in fading channels is to express the performance in terms of the Q-function with an instantaneous signal-to-noise ratio (SNR). We consider independent fading with either the unit average power or the average power of h^p considering the propagation path-loss effect in Eq. (1). We assume perfect channel state information (CSI) at relays and at the destination.

a) One relayed branch with two hops: The probability of a bit error of the relayed transmission with the instantaneous fading power x and y from S to R and R to D, respectively, at a high SNR can be written as [3]

$$P_b \approx \int_0^\infty \int_0^\infty Q\left(\sqrt{\frac{xy}{x+y}\bar{\gamma}}\right) f_x(x) f_y(y) dx dy \tag{3}$$

where $\bar{\gamma} = P_x/\sigma^2$ is the average SNR, $\bar{\gamma} = 2\bar{\gamma}_b$ for binary phase-shift keying (BPSK), and $\bar{\gamma}_b = E_b/N_o$ where E_b is the bit energy. Moreover $f_x(x)$ and $f_y(y)$ are the fading PDF in

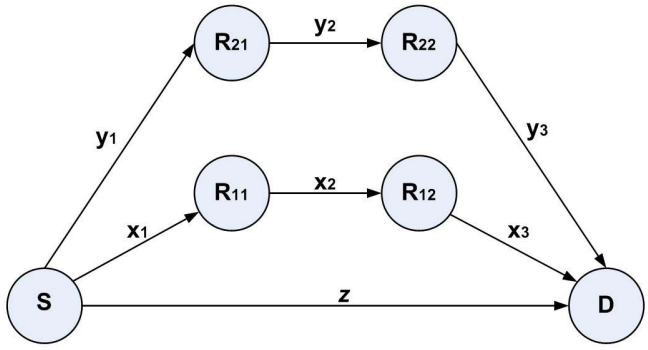

Fig. 1. CD with three branches (n=3) and three hops (h=3): Source (S), Relays (R) and Destination (D).

Manuscript received September 1, 2010; revised December 9, 2010, February 7, 2011, and April 2, 2011; accepted April 4, 2011. The associate editor coordinating the review of this letter and approving it for publication was M. Morelli.

The author is with the University of Nebraska - Lincoln, Omaha, NE 68182 (e-mail: wjang1@unl.edu).

Digital Object Identifier 10.1109/TWC.2011.050511.101560

1536-1276/11$25.00 © 2011 IEEE

each hop. As shown in Appendix A, we can rewrite the BER as

$$P_b \approx \int_0^\infty Q\left(\sqrt{x\bar{\gamma}}\right) f_x(x)dx + \int_0^\infty Q\left(\sqrt{y\bar{\gamma}}\right) f_y(y)dy \quad (4)$$

$$= 2\int_0^\infty Q\left(\sqrt{x\bar{\gamma}}\right) f_x(x)dx \quad (5)$$

where we assume $f_x(x) = f_y(y)$. With a change of variable ($\rho = x\bar{\gamma}$), we obtain $Q(\sqrt{x}) \doteq \frac{1}{2}\delta(x-2)$ as shown in Appendix B. The Q-function approximation of a delta impulse is crucial in our paper and the basis of our proposed CD analysis method. With this result, we find that

$$P_b \doteq 2\int_0^\infty Q\left(\sqrt{\rho}\right) f_x\left(\frac{\rho}{\bar{\gamma}}\right)\frac{1}{\bar{\gamma}}d\rho = 2\int_0^\infty \frac{1}{2}\delta(\rho-2) \quad (6)$$

$$f_x\left(\frac{\rho}{\bar{\gamma}}\right)\frac{1}{\bar{\gamma}}d\rho = f_x\left(\frac{2}{\bar{\gamma}}\right)\frac{1}{\bar{\gamma}} \quad (7)$$

where the symbol '$\doteq$' is used to denote the approximation due to sampling while '$\approx$' indicates general approximation in the context. For example, in Rayleigh fading channels we have $f_x(x) = e^{-x}$, which is simply obtained by letting m=1 in the expression of the Nakagami-m fading in Eq. (23). Since $\bar{\gamma} = 2\bar{\gamma}_b$ for BPSK,

$$P_b \doteq \frac{1}{\bar{\gamma}} f_x\left(\frac{2}{\bar{\gamma}}\right) = \frac{1}{\bar{\gamma}}\exp\{-2/\bar{\gamma}\} = \frac{1}{2\bar{\gamma}_b}\exp\{-1/\bar{\gamma}_b\} \quad (8)$$

$$= \frac{1}{2\bar{\gamma}_b}\sum_{k=0}^{\infty}\frac{(-1)^k}{k!}\bar{\gamma}_b^{-k} \approx \frac{1}{2\bar{\gamma}_b} \quad (9)$$

where the approximation is introduced to represent the BER at a high SNR, which is the well known result for dual hop one branch Rayleigh fading channel in the literature [3, Eq. (40)]. In the general case, $f_x(x)$ and $f_y(y)$ may not be the same PDF. Then,

$$P_b \doteq f_x\left(\frac{2}{\bar{\gamma}}\right)\frac{1}{2\bar{\gamma}} + f_y\left(\frac{2}{\bar{\gamma}}\right)\frac{1}{2\bar{\gamma}}. \quad (10)$$

b) Three branches (one direct path and two relayed paths each with three hops): The probability of a bit error at a high SNR for the cooperative transmission shown in Fig. 1 can be expressed as shown in Eq. (11) where $\bar{\gamma}$ and $\bar{\gamma}_z$ are the average SNR at the relays and the direct path respectively. With identical fading in each branch, i.e., $f_{x_1}(x_1) = f_{x_2}(x_2) = f_{x_3}(x_3)$ and $f_{y_1}(y_1) = f_{y_2}(y_2) = f_{y_3}(y_3)$, we have

$$P_b \doteq 3^2\int_{x_1=0}^\infty\int_{y_1=0}^\infty\int_{z=0}^\infty Q\left(\sqrt{x_1\bar{\gamma}+y_1\bar{\gamma}+z\bar{\gamma}_z}\right) f_{x_1}(x_1)f_{y_1}(y_1)f_z(z)dx_1dy_1dz. \quad (12)$$

To obtain Eq. (12), we applied the approximation of $Q(x) \approx \frac{1}{2}\mathrm{e}^{-x^2/2}$ to Eq. (11). Then we can separate Eq. (11) into three factors and apply Eq. (49) in Appendix A separately to each factor. Finally we can combine the three factors back into the Q-function in Eq. (12). Now we apply $Q(x) \approx \frac{1}{\sqrt{2\pi}x^2}\mathrm{e}^{-x^2/2}$ [10] to obtain

$$P_b \approx 3^2\int_{x_1=0}^\infty\int_{y_1=0}^\infty\int_{z=0}^\infty \frac{1}{\sqrt{2\pi\left(x_1\bar{\gamma}+y_1\bar{\gamma}+z\bar{\gamma}_z\right)}} \exp\{-x_1\bar{\gamma}/2\}\exp\{-y_1\bar{\gamma}/2\}\exp\{-z\bar{\gamma}_z/2\} f_{x_1}(x_1)f_{y_1}(y_1)f_z(z)dx_1dy_1dz. \quad (13)$$

With change of variables ($x_1\bar{\gamma} = x$, $y_1\bar{\gamma} = y$ and $z\bar{\gamma}_z = w$), we obtain

$$P_b \doteq 3^2\int_{x=0}^\infty\int_{y=0}^\infty\int_{w=0}^\infty \frac{1}{\sqrt{2\pi\left(x+y+w\right)}} \exp\{-x/2\}\exp\{-y/2\}\exp\{-w/2\} f_{x_1}\left(\frac{x}{\bar{\gamma}}\right) f_{y_1}\left(\frac{y}{\bar{\gamma}}\right) f_z\left(\frac{w}{\bar{\gamma}_z}\right)\frac{1}{\bar{\gamma}^2}\frac{1}{\bar{\gamma}_z}dxdydw. \quad (14)$$

Following the same process in Appendix B, we can obtain $\frac{1}{2}\mathrm{e}^{-x/2} \doteq \delta(x-2)$. Therefore, we find

$$P_b \doteq \frac{2^3 3^2}{\sqrt{2\pi\left(2+2+2\right)}} f_{x_1}\left(\frac{2}{\bar{\gamma}}\right) f_{y_1}\left(\frac{2}{\bar{\gamma}}\right) f_z\left(\frac{2}{\bar{\gamma}_z}\right)\frac{1}{\bar{\gamma}^2}\frac{1}{\bar{\gamma}_z}. \quad (15)$$

c) Cooperative system with n-branches and h-hops: We can generalize the result to n-branches (including the direct path) with h-hops in each relayed branch as

$$P_b \doteq \frac{2^n h^{n-1}}{\sqrt{2\pi 2n}} f_z\left(\frac{2}{\bar{\gamma}_z}\right)\frac{1}{\bar{\gamma}_z}\prod_{i=1}^{n-1}\left[f_i\left(\frac{2}{\bar{\gamma}}\right)\frac{1}{\bar{\gamma}}\right] \quad (16)$$

where $f_i(\cdot)$ is the PDF of the fading in the i-th relayed branch if we assume that the fading is identical in each hop in the same branch. The average received SNR at relays is $\bar{\gamma} = 2\bar{\gamma}_b h^p$ if we consider the propagation path-loss effect with the path-loss exponent of p and equally spaced relays between S and D. $\bar{\gamma}_z = 2\bar{\gamma}_b$ is the average SNR in the direct path. We can extend the result to n-branches with h_j-hops in the j-th relayed branch with different fading in each hop as

$$P_b \doteq \frac{2^n}{\sqrt{2\pi 2n}}\frac{f_z(2/\bar{\gamma}_z)}{\bar{\gamma}_z}\sum_{i_1=1}^{h_1}\sum_{i_2=1}^{h_2}\cdots \sum_{i_{n-1}=1}^{h_{n-1}}\frac{f_{i_1}(2/\bar{\gamma}_{i_1})}{\bar{\gamma}_{i_1}}\frac{f_{i_2}(2/\bar{\gamma}_{i_2})}{\bar{\gamma}_{i_2}}\cdots\frac{f_{i_{n-1}}(2/\bar{\gamma}_{i_{n-1}})}{\bar{\gamma}_{i_{n-1}}} \quad (17)$$

where $\bar{\gamma}_{i_j}$ is the average SNR at the j-th relayed branch, each with different number of hops.

d) Diversity Order and Coding Gain: The diversity order and coding gain for the average error rate depend on the fading PDF. Considering Rayleigh fading in Eq. (16), we have

$$P_b \doteq \frac{2^n h^{n-1}}{\sqrt{2\pi 2n}}\exp\{-2/\bar{\gamma}_z\}\frac{1}{\bar{\gamma}_z}\left[\exp\{-2/\bar{\gamma}\}\frac{1}{\bar{\gamma}}\right]^{n-1}. \quad (18)$$

Applying $\bar{\gamma}_z = 2\bar{\gamma}_b$ and $\bar{\gamma} = 2\bar{\gamma}_b h^p$ for BPSK with the propagation path-loss effect leads to Eqs. (19) to (22) where we applied the power series expansion. For a large SNR, the first term in the series will dominate and can be used to define the diversity order and coding gain [11]. Therefore, for the cooperative network of h hops and n branches with Rayleigh fading channels, the diversity order is n and the coding gain is $\left(4\pi n\, h^{2(p-1)(n-1)}\right)^{1/(2n)}$, where p is the path-loss exponent.

Now, we consider Nakagami-m fading PDF to obtain the diversity order and coding gain. The PDF of the Nakagami-m fading channel is given by [11]

$$f(x) = \frac{m^m x^{m-1}}{\Gamma(m)}\exp\{-mx\}, \quad x \geq 0. \quad (23)$$

The mean of the fading PDF is the unity regardless of the fading parmater m [14], which makes the average received power with fading the same as that of without fading. We assume the same fading parameter at the direct and relayed paths. Then, using Eq. (16) we get

$$P_b \doteq \frac{2^n h^{n-1}}{\sqrt{2\pi 2n}} \left[\frac{m^m}{\Gamma(m)} \left(\frac{2}{\bar{\gamma}} \right)^{m-1} \exp\{-2m/\bar{\gamma}\} \frac{1}{\bar{\gamma}} \right]^n \quad (24)$$

$$\approx \left[(4\pi n)^{1/(2mn)} h^{-(n-1)/(mn)} \Gamma(m)^{1/m} m^{-1} \bar{\gamma}_b \right]^{-nm} \quad (25)$$

with BPSK and without considering the propagation path-loss effect. The approximation is introduced since $e^{-2m/\bar{\gamma}} \approx 1$ at a high SNR. Therefore, for the cooperative network of h hops and n branches with Nakagami-m fading channels, the diversity order is nm and the coding gain is $(4\pi n)^{1/(2mn)} h^{-(n-1)/(mn)} \Gamma(m)^{1/m} m^{-1}$. From Eqs. (22) and (25), we can see that the number of branches relates to the diversity order while the number of hops determines the coding gain.

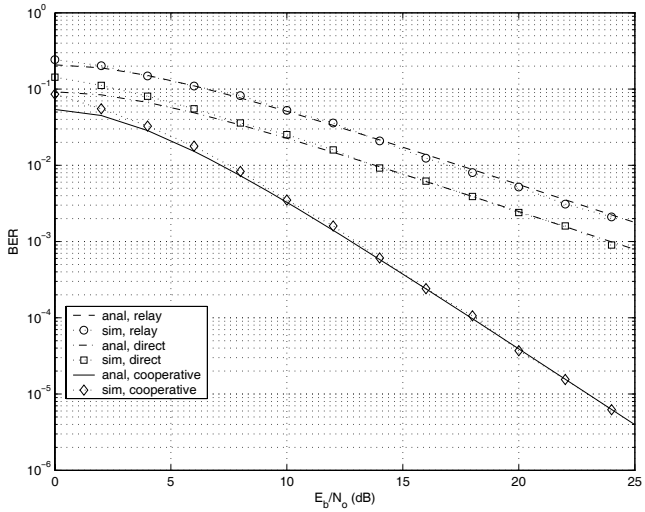

Fig. 2. Analytical and simulated BER, relayed, direct and cooperative transmission, n=2, h=2, $\bar{\gamma} = 2E_b/N_o$, Rayleigh.

III. Numerical Results

a) Examples: We employ Rayleigh fading channels in Figs. 2 to 4. The noise power is normalized before MRC in the simulation. Fig. 2 displays the analytical and simulated BER of the direct, relayed, and cooperative transmission without considering the propagation path-loss effect. We can see how cooperative diversity is achieved compared to the direct transmission. In Fig. 3, the performance of the relayed transmission is displayed with two, six and ten hops. The propagation path-loss exponent of three is considered to reflect suburban areas. Therefore, the average SNR at relays is equal to $2h^3 E_b/N_o$. As the number of hops increases, the performance improvement is significant up to six hops. After that, the performance enhancement rate is moderate as more hops are added. Analytical and simulated BER agree well in Figs. 2 and 3. In fact, the delta sampling BER is more accurate than [3, Fig. 7] at a low SNR as shown in Fig. 2. Cooperative diversity is evident in Fig. 4 where the same path-loss exponent is employed. The diversity order and coding gain in Eq. (22) is also plotted. We can see that cooperative diversity increases as the number of branches increases while the coding gain increases with the number of hops. The analytical BER in Eq. (16) agrees with simulation results at a moderate and high SNR, and a similar effect was also observed in [3]. Fig. 5 displays a mixed fading scenario where the direct path experiences a Rayleigh fading while the relayed paths undergo Rician fadings (Nakagami-n with n=1). The BER of CD with two, three and four branches is displayed assuming independent fading with the unit average power in each hop without considering the propagation path-loss effect in Eq. (1). The proposed analytical BER represents the simulated BER well. With the same network in Fig. 5, Nakagami-m fading performance is now displayed in Fig. 6 with the fading parameter, m=2. Analytical BER is obtained using Eq. (16). The diversity order and coding gain in Eq. (25) agree well with the simulated BER at a high SNR. From Figs. 5 and 6, we observe that the analytical BER tends to be optimistic as the number of branches increases.

$$P_b \approx \int_{x_1=0}^{\infty} \cdots \int_{y_1=0}^{\infty} \cdots \int_{z=0}^{\infty} Q\left(\sqrt{\frac{x_1x_2x_3\bar{\gamma}}{x_1x_2 + x_2x_3 + x_1x_3} + \frac{y_1y_2y_3\bar{\gamma}}{y_1y_2 + y_2y_3 + y_1y_3} + z\bar{\gamma}_z} \right) f_{x_1}(x_1) f_{x_2}(x_2) f_{x_3}(x_3) f_{y_1}(y_1) f_{y_2}(y_2) f_{y_3}(y_3) f_z(z) dx_1 \ldots dy_1 \ldots dz \quad (11)$$

$$P_b \doteq \frac{2^n h^{n-1}}{\sqrt{2\pi 2n}} \exp\{-2/(2\bar{\gamma}_b)\} \frac{1}{2\bar{\gamma}_b} \left[\exp\{-2/(2h^p\bar{\gamma}_b)\} \frac{1}{2h^p\bar{\gamma}_b} \right]^{n-1} \quad (19)$$

$$= \frac{h^{-(p-1)(n-1)}}{\sqrt{2\pi 2n}} \bar{\gamma}_b^{-n} \exp\{-(n + h^p - 1)/(h^p\bar{\gamma}_b)\} \quad (20)$$

$$= \frac{h^{-(p-1)(n-1)}}{\sqrt{2\pi 2n}} \bar{\gamma}_b^{-n} \sum_{i=0}^{\infty} \frac{(-1)^i (n + h^p - 1)^i}{i!(h^p\bar{\gamma}_b)^i} \approx \frac{h^{-(p-1)(n-1)}}{\sqrt{2\pi 2n}} \bar{\gamma}_b^{-n} \quad (21)$$

$$= \left[\left(4\pi n h^{2(p-1)(n-1)} \right)^{1/(2n)} \bar{\gamma}_b \right]^{-n} \quad (22)$$

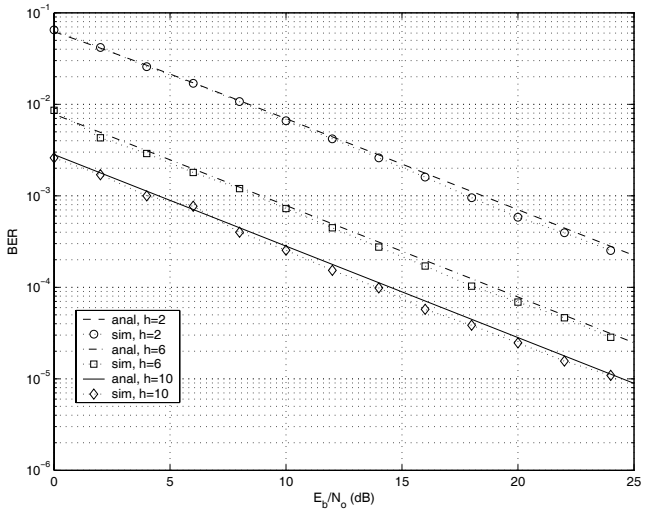

Fig. 3. Analytical and simulated BER, multi-hop relayed transmission, n=1, h=2,6,10, $\bar{\gamma} = 2h^3 E_b/N_o$, Rayleigh.

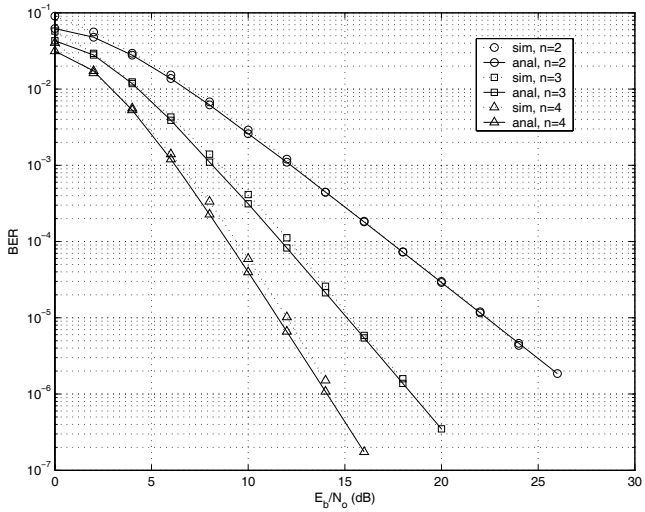

Fig. 5. Analytical and simulated BER, CD, mixed fadings, n=2,3,4, h=2, $\bar{\gamma} = 2E_b/N_o$, Rayleigh and Rician.

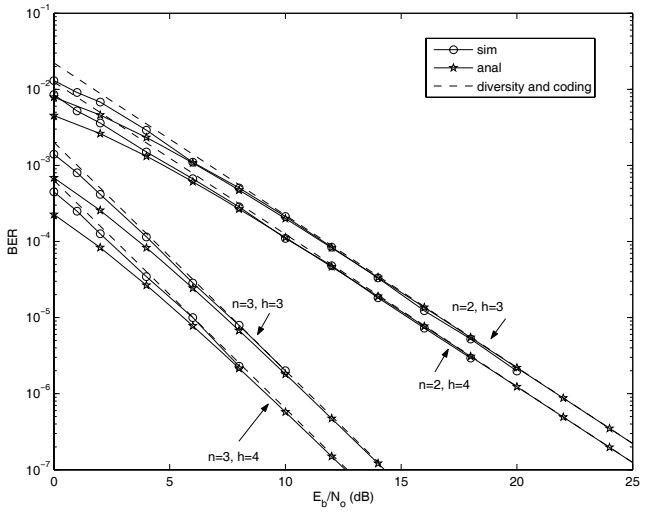

Fig. 4. Analytical and simulated BER, CD, n=2,3, h=3,4, $\bar{\gamma} = 2h^3 E_b/N_o$, Rayleigh.

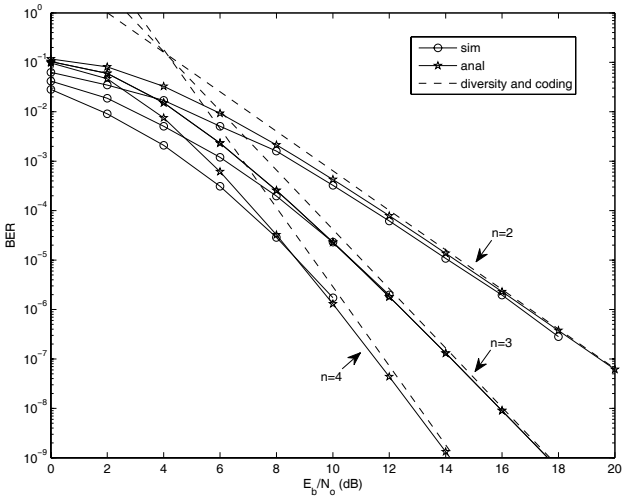

Fig. 6. Analytical and simulated BER, CD, n=2,3,4, h=2, m=2, $\bar{\gamma} = 2E_b/N_o$, Nakagami-m.

b) Accuracy Analysis: We choose Rayleigh fading for demonstration since the BER accuracy depends on the fading PDF in the channel. Applying the delta sampling to a Rayleigh fading channel with BPSK amounts to

$$P_b \doteq \int_0^\infty Q(\sqrt{x\bar{\gamma}}) \exp\{-x\} dx \tag{26}$$

$$= \int_0^\infty Q(\sqrt{\rho}) \exp\{-\rho/\bar{\gamma}\} \frac{1}{\bar{\gamma}} d\rho \tag{27}$$

$$= \frac{1}{2} \int_0^\infty \delta(\rho - 2) \exp\{-\rho/\bar{\gamma}\} \frac{1}{\bar{\gamma}} d\rho \tag{28}$$

$$= \frac{1}{2\bar{\gamma}} \exp\{-2/\bar{\gamma}\} \tag{29}$$

$$= \frac{1}{4\bar{\gamma}_b} \exp\{-1/\bar{\gamma}_b\} = \frac{1}{4\bar{\gamma}_b} \sum_{n=0}^{\infty} \frac{(-1)^n}{n!} \left(\frac{1}{\bar{\gamma}_b}\right)^n \tag{30}$$

$$\approx \frac{1}{4\bar{\gamma}_b}. \tag{31}$$

where approximation ('$\approx$') is introduced to represent the BER at a large SNR. The result is identical to [12, Eq. (14.3-13)]. However, the delta BER is smaller than the actual BER at a low SNR that can be seen in Fig. 4. We can also observe that the delta sampling BER is larger than the actual BER at a low SNR in Fig. 6 for Nakagami-m fading channels. Therefore, the delta approximation is neither an upper bound nor a lower bound. However, the delta approximation provides rather close estimation at a moderate or high SNR. We find that the analytical BER using the inequality between harmonic and geometric mean in [8, Fig. 2] is more accurate at a low SNR while ours is more accurate at a high SNR.

The overall fading effect of CD tends to be spread relative to the error function. Consequently, the proposed approach becomes more applicable to CD. Regarding the single-input and single-output (SISO) direct communication system, we can combine the error function and the fading PDF to obtain a delta impulse function for an accurate system performance analysis [13]. We observe that the analytical BER of CD using

sampling becomes optimistic as the diversity order increases. This is because the fading PDF approaches a delta impulse function faster than the error function does as N approaches infinity. To obtain more accurate analytical BER of CD for a larger diversity order or at a low SNR, we can also combine the fading PDF and the Q-function to obtain a delta impulse function for sampling.

IV. Conclusion

We proposed a simple and general approach to evaluating the performance of amplify-and-forward cooperative diversity using the sampling property of a delta function. The Q-function approaches to a delta impulse function asymptotically. We showed that the sampling method can be applied to cooperative networks with mixed fading to obtain the system performance. The simulation results agree well with the analytical results at a moderate or high SNR and with a practical diversity order.

Appendix A

Decoupling of the Q-function in a multi-hop relayed transmission: Let us define the double integral g as

$$g := \int_0^\infty \int_0^\infty Q\left(\sqrt{\frac{xy}{x+y}}\right) f_x(x) f_y(y) dx dy. \tag{32}$$

With a change of variables ($x = t^N$ and $y = u^N$ as $N \to \infty$), we have Eqs. (33) and (34) where $h(t^N, u^N)$ is defined as

$$h(t^N, u^N) := \Psi\left(t^N, u^N\right) N t^{N-1} N u^{N-1} \tag{35}$$

with

$$\Psi(t^N, u^N) := Q\left(\sqrt{\frac{t^N u^N}{t^N + u^N}}\right) \tag{36}$$

$$= Q\left(\sqrt{\left(\frac{1}{t^N} + \frac{1}{u^N}\right)^{-1}}\right). \tag{37}$$

We can consider four different cases depending on the values of t^N and u^N as shown in Eqs. (38) to (41) where the last case is negligible compared to the second and third cases. Since $0 \le \Psi(t^N, u^N) \le 0.5$, the value of $h(t^N, u^N)$ largely depends on the value of t^N and u^N. Therefore, Eq. (35) can be rewritten as

$$h(t^N, u^N) \approx \lim_{u^N \to \infty} h(t^N, u^N) + \lim_{t^N \to \infty} h(t^N, u^N) \tag{42}$$

$$= Q\left(\sqrt{t^N}\right) N t^{N-1} N u^{N-1} + Q\left(\sqrt{u^N}\right) N t^{N-1} N u^{N-1}. \tag{43}$$

Then, the double integral of the first term in Eq. (43) becomes

$$\int_0^\infty Q\left(\sqrt{t^N}\right) f_x(t^N) N t^{N-1} dt \int_1^\infty f_y(u^N) N u^{N-1} du \tag{44}$$

where the lower limit of the second integration is one since $\lim_{N\to\infty} u^N = \infty$. We can change the lower limit to zero since $\lim_{N\to\infty} u^{N-1} = 0$ for $0 \le u < 1$. Then, Eq. (44) can be rewritten as

$$\int_0^\infty Q\left(\sqrt{t^N}\right) f_x(t^N) N t^{N-1} dt \int_0^\infty f_y(u^N) N u^{N-1} du \tag{45}$$

$$= \int_0^\infty Q\left(\sqrt{x}\right) f_x(x) dx. \tag{46}$$

Therefore, the double integral g can be decoupled into

$$g \approx \int_0^\infty Q\left(\sqrt{x}\right) f_x(x) dx + \int_0^\infty Q\left(\sqrt{y}\right) f_y(y) dy. \tag{47}$$

We can extend the result to the h-hop relayed branch to decouple g_h as

$$g_h \approx \int_0^\infty \cdots \int_0^\infty Q\left(\sqrt{\frac{\prod_{i=1}^h x_i}{\sum_{j=1}^h \prod_{\substack{l=1 \\ l\neq j}}^h x_l}}\right) f_{x_1}(x_1) \ldots f_{x_h}(x_h) d_{x_1} \ldots d_{x_h} \tag{48}$$

$$= \sum_{i=1}^h \int_0^\infty Q(\sqrt{x_i}) f_{x_i}(x_i) d_{x_i}. \tag{49}$$

Appendix B

Asymptotic delta function of the Q-function: Let us define the integral g as

$$g := \int_0^\infty Q(\sqrt{x}) f(x) dx. \tag{50}$$

With a change of variable ($x = t^N$ as $N \to \infty$),

$$g = \int_0^\infty Q(\sqrt{t^N}) f(t^N) N t^{N-1} dt = \int_0^\infty h(t^N) f(t^N) dt \tag{51}$$

where $h(t^N)$ is defined as

$$h(t^N) := Q(\sqrt{t^N}) N t^{N-1}. \tag{52}$$

We observe that the area of $h(t^N)$,

$$a = \int_0^\infty h(t^N) dt = \int_0^\infty Q(\sqrt{x}) dx = \frac{1}{2}. \tag{53}$$

To find the critical point of $h(t^N)$, we employ Leibnitz differentiation rule [14]. Then,

$$\frac{dh(t^N)}{dt} = -\frac{1}{2}\left(t^N\right)^{-\frac{1}{2}} N t^{N-1} \frac{1}{\sqrt{2\pi}} \exp\{-t^N/2\} N t^{N-1} + Q\left(\sqrt{t^N}\right) N(N-1) t^{N-2} = 0. \tag{54}$$

Applying $Q(x) \approx \frac{1}{\sqrt{2\pi x^2}} \mathrm{e}^{-x^2/2}$ [10] to Eq. (54), we obtain the critical point as $N \to \infty$:

$$t_*^N = \lim_{N\to\infty} \frac{2(N-1)}{N} = 2. \tag{55}$$

From Eq. (54), we can also see that $dh(t^N)/dt > 0$ for $0 \le t^N < t_*^N$, and $dh(t^N)/dt < 0$ for $t^N > t_*^N$. Therefore, we found that $h(t^N)$ is a unimodal function with its maximum at t_*^N. From Eq. (52), we can show that

$$\lim_{N\to\infty} h(t_*^N) = \lim_{N\to\infty} 2NQ\left(\sqrt{2}\right) = \infty. \tag{56}$$

With the result of Eq. (56) together with Eqs. (53) and (55), we can state that

$$\lim_{N\to\infty} h(t^N) = \frac{1}{2}\delta\left(t^N - 2\right). \tag{57}$$

$$g = \int_0^\infty \int_0^\infty Q\left(\sqrt{\frac{t^N u^N}{t^N + u^N}}\right) f_x(t^N) f_y(u^N) N t^{N-1} N u^{N-1} dt du \tag{33}$$

$$= \int_0^\infty \int_0^\infty h(t^N, u^N) f_x(t^N) f_y(u^N) dt du \tag{34}$$

$$\lim_{\substack{t^N \to \infty \\ u^N \to \infty}} \Psi(t^N, u^N) = 0 \text{ and } \lim_{\substack{t^N \to \infty \\ u^N \to \infty}} h(t^N, u^N) = 0 \tag{38}$$

$$\lim_{\substack{t^N \to \infty \\ u^N < \infty}} \Psi(t^N, u^N) = Q\left(\sqrt{u^N}\right) \text{ and } \lim_{\substack{t^N \to \infty \\ u^N < \infty}} h(t^N, u^N) > 0 \tag{39}$$

$$\lim_{\substack{t^N < \infty \\ u^N \to \infty}} \Psi(t^N, u^N) = Q\left(\sqrt{t^N}\right) \text{ and } \lim_{\substack{t^N < \infty \\ u^N \to \infty}} h(t^N, u^N) > 0 \tag{40}$$

$$\lim_{\substack{t^N < \infty \\ u^N < \infty}} \Psi(t^N, u^N) > 0 \text{ and } \lim_{\substack{t^N < \infty \\ u^N < \infty}} h(t^N, u^N) > 0 \tag{41}$$

Now, Eq. (51) becomes

$$g \doteq \frac{1}{2} \int_0^\infty \delta\left(t^N - 2\right) f(t^N) dt \tag{58}$$

$$= \frac{1}{2} f(2) \int_0^\infty \delta\left(t^N - 2\right) dt \tag{59}$$

where we applied the multiplication property of the delta function. Here we assume that $f(t^N)$ does not go to a delta impulse function as fast as $h(t^N)$ does as N approaches infinity. From Eqs. (57) and (52), we find

$$\delta(t^N - 2) = \lim_{N \to \infty} 2h(t^N) = \lim_{N \to \infty} 2Q(\sqrt{t^N}) N t^{N-1} \tag{60}$$

and using Eq. (53)

$$\int_0^\infty \delta\left(t^N - 2\right) dt = 1. \tag{61}$$

Therefore,

$$g = \int_0^\infty Q(\sqrt{x}) f(x) dx \doteq \frac{1}{2} f(2). \tag{62}$$

Consequently, the Q-function in Eq. (50) becomes a delta function asymptotically:

$$Q(\sqrt{x}) \doteq \frac{1}{2} \delta\left(x - 2\right). \tag{63}$$

REFERENCES

[1] J. N. Laneman, D. N. C. Tse, and G. W. Wornell, "Cooperative diversity in wireless network efficient protocols and outage behavior," *IEEE Trans. Inf. Theory*, vol. 50, no. 12, pp. 3062-3080, Dec. 2004.

[2] A. Sendonaris, E. Erkip, and B. Aazhang, "User cooperation diversity–part II: implementation aspects and performance analysis," *IEEE Trans. Commun.*, vol. 51, no. 11, pp. 1939-1948, Nov. 2003.

[3] A. Ribeiro, X. Cai, and G. B. Giannakis, "Symbol error probabilities for general cooperative links," *IEEE Trans. Wireless Commun.*, vol. 4, no. 3, pp. 1264-1273, May 2005.

[4] M. O. Hasna and M-S. Alouini, "Harmonic mean and end-to-end performance of transmission system with relays," *IEEE Trans. Commun.*, vol. 52, no. 1, pp. 130-135, Jan. 2004.

[5] G. K. Karagiannidis, T. A. Tsiftsis, and R. K. Malik, "Bounds of multihop relayed communications in Nakagami-m fading," *IEEE Trans. Commun.*, vol. 54, no. 1, pp. 18-22, Jan. 2006.

[6] S. Ikki and M. H. Ahmed, "Performance analysis of cooperative diversity wireless networks over Nakagami-m fading channel," *IEEE Commun. Lett.*, vol. 11, no. 4, pp. 334-336, Apr. 2007.

[7] S. Ikki and M. H. Ahmed, "Performance of decode-forward cooperative diversity networks over Nakagami-m fading channels," in *Proc. IEEE Global Telecommun. Conf.*, pp. 4328-4333, Nov. 2007.

[8] T. A. Tsiftsis, G. K. Karagiannidis, S. A. Kotsopoulos, and F.-N. Pavlidou, "BER analysis of collaborative dual-hop wireless transmissions," *IET Electron. Lett.*, vol. 40, no. 11, May 2004.

[9] T. A. Tsiftsis, G. K. Karagiannidis, P. T. Mathiopoulos, and S. A. Kotsopoulos, "Nonregenerative dual-hop cooperative links with selection diversity," *EURASIP J. Wireless Commun. Netw.*, article ID 17862, 2006.

[10] J. M. Wozencraft and I. M. Jacobs, *Principles of Communication Engineering*, pp. 83. John Wiley & Sons, 1965.

[11] Z. Wang and G. B. Giannakis, "A simple and general parameterization quantifying performance in fading channels," *IEEE Trans. Commun.*, vol. 51, no. 8, pp. 1389-1398, Aug. 2003.

[12] J. G. Proakis, *Digital Communications*, 4th edition, pp. 819. McGraw Hill, 2001.

[13] W. M. Jang, "Quantifying performance in fading channels using the sampling property of a delta function," *IEEE Commun. Lett.*, vol. 15, no. 3, pp. 266-268, Mar. 2011.

[14] A. Papoulis and S. U. Pillai, *Probability, Random Variables, and Stochastic Processes*, 4th edition. McGraw-Hill, 2002.